Relativistic Density Functional Study of the Dinuclear Uranyl Complex $[(UO_2)_2(\mu_2\text{-}OH)_2Cl_2(H_2O)_4]$ in Its Crystalline Environment

Florian Schlosser,[a] Sven Krüger,[a] and Notker Rösch*[a]

Keywords: Actinides / Uranium / Hydrogen bonds / Relativistic density functional calculations

The hexavalent dinuclear uranyl dichloride complex $[(UO_2)_2(\mu_2\text{-}OH)_2Cl_2(H_2O)_4]$ was studied computationally with an all-electron scalar relativistic density functional method. This suggested hydrolysis product of uranyl in the presence of chlorine ions is one of the few polynuclear uranyl species for which a crystal structure is known. The calculated gas-phase structure is similar to the experimental crystal geometry; any major deviations are due to hydrogen bonds in the crystal. If the eight strongest hydrogen bonds are included in a model of the complex's crystalline environment, the calculated structure improves significantly. Based on this model, the hydrogen bond lengths and angles were determined, indicating that they are moderate and strong with an average binding energy of 39 kJ/mol. These computational results corroborate earlier suggestions based on experimental results concerning the location and strength of the hydrogen bonds. In addition, a valuable reference for relativistic quantum chemical methods is provided by the gas-phase results.

Introduction

The dinuclear complex $[(UO_2)_2(\mu_2\text{-}OH)_2Cl_2(H_2O)_4]$ (**1**) has been discussed as a polynuclear species in the initial phase of uranyl hydrolysis in the presence of chlorine ions.[1,2] While structural information about such polynuclear actinide complexes is rare, data are available from EXAFS studies that refer directly to the species in solution or from a crystal structure determination if a crystal can be grown from solution.[3−5] X-ray scattering data of a solution[1] and a crystal structure[2] determined for **1** from hydrolyzed solutions of $UO_3{\cdot}HCl{\cdot}2H_2O$ indicate the presence of the dimeric unit $(UO_2)_2(\mu_2\text{-}OH)_2^{2+}$, which has also been reported in other crystal structures.[3−5] This moiety seems to be an important structural element of dinuclear uranium species in the solid state and in solution.

Recent developments in quantum chemistry[6−12] have rendered relativistic electronic structure calculations feasible for larger compounds of very heavy elements such as the actinides and have, therefore, opened up a computational route to many of their properties. Electronic correlation as well as relativistic effects substantially affect the electronic structure of heavy-element compounds, and therefore have to be accounted for in a correct description of such systems.[13] In addition, the large number of electrons of these elements demands an efficient computational method, so that one is not restricted to small or highly symmetric model species. This renders methods based on density functional (DF) theory very attractive.

Our first goal was to describe the gas-phase structure of the title complex **1** using an appropriate all-electron scalar relativistic DF approach[7,14] that combines a geometry optimization using a local-density approximation (LDA) of the exchange-correlation functional and an energy evaluation using a generalized-gradient approximation (GGA, see Computational Details). In a second step, we modeled the packing effects in the crystal structure of **1** and compared this model with available experimental data.[2] Because **1** is neutral, long-range Coulomb interactions between the different units in the crystal should not be crucial; rather, one expects that hydrogen bonds comprise the main crystal packing effects.[2] Therefore, we chose a model approach which neglects the Madelung field. To the best of our knowledge, this work is the first attempt to model crystal packing effects of a dinuclear actinide species in a quantum chemistry investigation. Even with its simplifications, this model study represents a major challenge to the scalar relativistic DF method applied.

In the next section, we describe details of the crystal structure and present the models chosen to describe complex **1**. We then discuss results for geometry and energetics of **1** and details of the calculated hydrogen bonds, and compare the different models with experimental data. Finally, we provide computational details.

[a] Institut für Physikalische und Theoretische Chemie, Technische Universität München,
Lichtenbergstr. 4, 85747 Garching, Germany
Fax: (internat.) + 49-89/289-13468
E-mail: roesch@ch.tum.de

Supporting information for this article is available on the WWW under http://www.eurjic.org or from the author.

  DOI: 10.1002/ejic.200300024

Crystal Structure and Models

Crystals of the diuranyl hydroxide dichloride complex $[(UO_2)_2(\mu_2\text{-}OH)_2Cl_2(H_2O)_4]$ (**1**) are monoclinic with a unit cell containing four formula units and belong to space group $P2_1/n$ (no. 14).[2] Complex **1** consists of two linear uranyl groups linked by two OH bridges, with the bridging oxygen centers denoted O_b. Both uranium centers are also surrounded by one chlorine and two further oxygen centers O_s and O_a due to coordinating aqua ligands. The index s designates O centers of aqua ligands located *syn* relative to a Cl ligand, while the index a refers to O centers of aqua ligands located *anti*, i.e. at the same uranium center, but on the side opposite to Cl (Figure 1). The two chlorine atoms, one at each U center, are *trans*-coordinated. Overall each U center is locally coordinated as a pentagonal bipyramid, which is typical for uranyl moieties.[15] The central unit $(UO_2)_2(\mu_2\text{-}OH)_2^{2+}$ is also present in the dinuclear hydrolysis product $[(UO_2)_2(\mu_2\text{-}OH)_2(H_2O)_6]^{2+}$ where the chlorine atoms are replaced by aqua ligands.[1] Although both OH and O bridges may be possible in the diuranyl species[16] previous studies[14] confirmed the presence of OH bridges at acidic pH in the initial stage of hydrolysis.

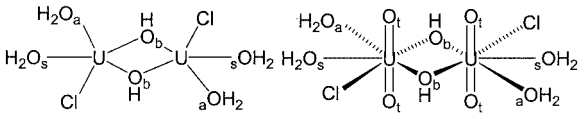

Figure 1. Schematic structure of the dinuclear complex $[(UO_2)_2(\mu_2\text{-}OH)_2Cl_2(H_2O)_4]$ (**1**): top view (left) and side-view (right); the terminal oxygen atoms of the uranyl units are not shown in the top view

Naturally, X-ray scattering data of the crystal structure do not provide explicit information about the positions of the hydrogen atoms. However, based on typical distances and angles found in the crystal structure, Åberg predicted three types of H bonds, X−H···Y, between adjacent complexes **1** (Figure 2).[2] The four strongest, i.e. shortest, bonds (A, B), extending in the *b* direction of the crystal, are assumed to exist between an oxygen center of an OH bridge and an oxygen center of an *anti*-coordinated aqua ligand, $O_b\cdots H-O_a$ (A) and $O_a-H\cdots O_b$ (B). (Frontier groups of an adjacent complex **1** are designated in *italics*.) Åberg predicted eight additional H bonds oriented mainly in the *c* direction.[2] Each of the first four H bonds (C, D) involves the same water oxygen center as H bond B and a chlorine center, $O_a-H\cdots Cl$ (C) and $Cl\cdots H-O_a$ (D); the second four H bonds (E, F) involve a bridging oxygen atom and a terminal uranyl oxygen atom, $O_t\cdots H-O_b$ (E) and $O_b-H\cdots O_t$ (F) (Figure 2). From a comparison of the corresponding X···Y distances with typical values for H bonds[17] and the van der Waals radii of the corresponding atoms,[18] we expect the bond strengths to decrease from (A, B) to (C, D) to (E, F).[2]

To determine the structure of complex **1**, we applied two models with C_i symmetry: M1 − a model of the gas-phase structure, and, to account for packing effects of the crystal,

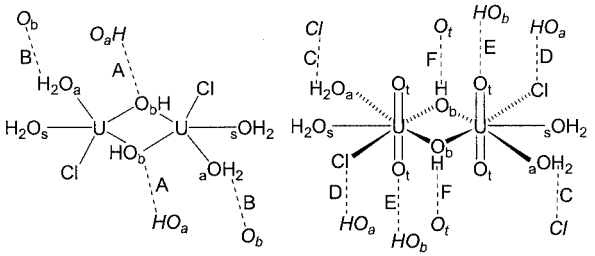

Figure 2. Schematic structure of the dinuclear complex $[(UO_2)_2(\mu_2\text{-}OH)_2Cl_2(H_2O)_4]$ (**1**), including the proposed H bonds A, B, C, D, E, and F in the crystal; see text; top view (left) and side-view (right); terminal oxygen atoms of the uranyl units are not shown in the top view; *italics* indicate frontier groups of neighboring complexes **1** in the crystal

M2 − a model including important features of the crystalline environment.

The C_i symmetry of M1 does not constrain any degree of freedom for a geometry optimization of **1**. The experimental crystal structure shows slight deviations from C_i symmetry because the local inversion symmetry of **1** is broken by the arrangement of the neighboring complexes: equivalent bond lengths scatter on average by 0.02 Å.[2] In addition, the crystal structure reveals that complex **1** exhibits approximately C_{2h} symmetry if H atoms are ommited.[2] Thus, to reduce the computational effort, we also used a model M0 with overall C_{2h} symmetry to generate a starting geometry for M1. In model M0, the OH bridges are coplanar with the $U-O_b-U-O_b$ plane and the coordinated water molecules are oriented symmetrically to this plane; these restrictions are released in model M1. To investigate the effect of the crystal hydrogen bonds on the gas-phase structure of model M1 we constructed model M2. Here, we place the gas-phase complex obtained with model M1 into a model of its crystalline environment and investigate the relaxation of the complex due to the H bonds. Comparing the optimized structure of model M2 with the crystal structure, we can check if the model environment can reproduce the main effects of crystal packing.

To model the effect of H bonds with neighboring complexes in the crystal, we represented neighboring complexes **1** by those frontier groups involved in the H bonds discussed above (Figure 2). To keep model M2 neutral, we chose H_2O and HCl molecules as the corresponding counterparts. Only the heavy atoms (O, Cl) of these model groups were placed at fixed positions derived from the experimental crystal structure.[2] Thus, the optimizations represent a relaxation of **1** in the fixed framework of heavy frontier atoms of the surrounding species in the molecular crystal. The locations of the hydrogen centers of the model groups (hence also the orientations of the H bonds) were fully optimized, subject to inversion symmetry constraint. The Mulliken charges of the corresponding centers of O (−0.62 e) in H_2O and Cl (−0.24 e) in HCl are close to those of the corresponding atoms of **1** as calculated with reference model M1, namely −0.54 e for O_a and −0.34 e for Cl. Therefore, the chemical environment of **1** in model M2 should be sufficiently similar to that of the crystal.

Our initial, simple model of the environment accounted only for the strongest H bonds (A, B); as expected, this yielded improved distances and angles of atoms directly connected to the simulated bridges but the localized formation of these selected H bonds distorts other parts of the complex. Therefore, in model M2 we included both (A, B) and (C, D) H bonds, still applying C_i symmetry, so as to model the eight strongest out of twelve H bonds assumed to be present in the crystal. Neglect of the weak E and F bridges is supported by the good agreement of the UO_t distances with experiment in all our models, indicating only small effects of these H bonds on the strong UO_t bonds. Rotation of the complex **1** inside the "matrix" set up by the H bonds of the environment would result in further H bonds to the frontier groups of neighboring complexes; to prevent such artifacts, we constrained the equatorial ligand atoms of the uranyl groups in a plane, in agreement with the experimental crystal structure. This approximation was checked by examining the structure's relaxation (model M2′, see below), which led to changes in bond lengths of **1** of < 0.02 Å. Therefore, the following discussion will focus on model M2.

Results and Discussion

Geometry

Table 1 summarizes the calculated structures of the three models studied and compares these results with experiment. First, we shall discuss the gas-phase reference model M1. The central dimeric unit $(UO_2)_2(OH)_2^{2+}$ consists of two slightly different ($\Delta = 0.07$ Å) bonds $U-O_b$ of the bridging hydroxy groups between the uranyl units. The OH moieties show a longer bond $U-O_b$ (2.39 Å) to the uranyl where H_2O is their neighboring ligand and a shorter bond $U-O_b'$ (2.32 Å) close to a neighboring Cl ligand (Figure 1). The O_b-H bonds are bent 66.6° out of the central $U-O_b-U-O_b$ plane. The uranyl moieties of M1 are almost linear (176.7°), very close to the linear structure of a uranyl ion UO_2^{2+}. The terminal oxygen−uranium distances $U-O_t$ are significantly longer than in the corresponding gas-phase calculations of the bare uranyl ion UO_2^{2+} ($\Delta = 0.08$ Å) and even slightly longer than calculated for the solvated uranyl ion $[UO_2(H_2O)_5]^{2+}$ ($\Delta = 0.03$ Å).[19] Such bond elongation is due to increasing competition with other, equatorial ligands at the U center which bind more strongly than water (OH, Cl). For the gas-phase structure of the analogous dinuclear complex $(UO_2)_2(OH)_2(H_2O)_6^{2+}$, almost equal $U-O_t$ distances ($\Delta = -0.01$ Å) and an increased bending of the uranyl moieties (168.0°) have been calculated.[14]

The $U-O_a$, $U-O_s$ and U−Cl bonds are bent out of the $U-O_b-U-O_b$ plane by 15.9°, 0.9° and 6.2°, respectively. Therefore, the pentagonal-bipyramidal coordination of the U centers, which is typical of monomeric complexes,[15] is slightly distorted. The bonds to the aqua ligands $U-O_a$ and $U-O_s$ (2.49 Å) are slightly longer than uranium−water distances in mononuclear $UO_2(H_2O)_5^{2+}$ (2.42 Å) and dinuclear[14] species $(UO_2)_2(OH)_2(H_2O)_6^{2+}$ (2.46 Å) due to an increasing number of more strongly binding ligands. Also, the U−Cl distance (2.63 Å) indicates strong ligand bonding because it is relatively short compared to computational results for $[UO_2Cl_4]^{2-}$ where the U−Cl distances are elongated due to the competition of four strong bonds (2.68 Å). This latter result is in good agreement with EXAFS data for this complex in solution (2.67 Å)[20] while DF GGA calculations yield longer bonds, from 2.73 to 2.81 Å.[8]

As there are no experimental data for the gas phase, we compared the results of model M1 with X-ray data in solution, to obtain initial indications of solvation and crystal packing effects on geometry. Åberg has investigated solutions of hydrolyzed uranyl(VI) chloride with constant [U] (3 M) but varying OH/U ratio, i.e. the average number of OH groups per U atom (0−1.11).[1] We choose the ratio 1.11 for comparison, in agreement with the assumed structure of **1** that exhibits two U centers linked by two OH bridges. The experimental results correspond to the assumed pentagonal coordination, including one U−Cl bond [$n_r = 0.8(1)$ for

Table 1. Structure parameters (distances in Å, angles in °) of models M0 (C_{2h}), M1 (C_i), and M2 (C_i) of complex $[(UO_2)_2(\mu_2\text{-}OH)_2Cl_2(H_2O)_4]$ (**1**) in the gas phase (M0, M1) and in a model of the crystalline environment (M2); also shown are experimental values and deviations ΔMn ($n = 0, 1, 2$) of calculated quantities from the crystal structure; the last line provides the types of H bonds that directly affect the corresponding distances and angles (for the designations, see Figure 2 and text)

	U−U	$U-O_t$	$U-O_b$	$U-O_b'$	$U-O_a$	$U-O_s$	U−Cl	O_t-U-O_t	O_b-U-O_b	O_a-U-O_s	O_s-U-Cl
M0	3.785	1.792	2.254	2.332	2.463	2.495	2.700	168.7	68.8	74.8	70.5
M1	3.801	1.787	2.389	2.318	2.493	2.486	2.626	176.7	72.3	65.7	69.2
M2	3.875	1.790	2.352	2.343	2.421	2.497	2.661	174.9	68.7	68.4	68.6
Exp.[a]	3.94(0)	1.79(2)	2.40(2)	2.34(2)	2.39(2)	2.50(3)	2.75(1)	178.2(9)	67.0(7)	68.8(9)	73.4(8)
Exp.[b]	3.84(1)	1.76(1)	*2.40(1)*	*2.40(1)*	*2.40(1)*	*2.40(1)*	2.89(2)	−	−	−	−
Δ M0	−0.16	0.00	−0.15	−0.01	0.07	0.00	−0.05	−9.5	1.8	6.0	−2.9
Δ M1	−0.14	0.00	−0.01	−0.02	0.10	−0.01	−0.12	−1.5	5.3	−3.1	−4.2
Δ M2	−0.07	0.00	−0.05	0.00	0.03	0.00	−0.09	−3.3	1.7	−0.4	−4.8
H bonds		E, F	A, B, E, F	A, B, E, F	A, B, C, D		C, D	E, F	A, B, E, F	A, B, C, D	C, D

[a] Ref.[2], crystal structure (average values with respect to the assumed C_i symmetry; maximum scattering of 0.04 Å for distances and 1.7° for angles); reference for determining the deviations Δ = X(calc.) − X(exp.). [b] Ref.[1], solution (only *average* value for all equatorial U−O distances determined by experiment).

U−Cl, where n_r is the number of corresponding bonds per U atom) and four U−O bonds [n_r = 4.3(2)], i.e. two bonds to bridging hydroxy moieties and two bonds to coordinated water molecules (Figure 1). The latter four uranium−oxygen bonds U−O_b, U−O_b', U−O_a, and U−O_s from the first hydration sphere could not be separated by experiment[1] so that only an average distance is available (2.40 Å, Table 1).

The U−O_t distance of model M1 agrees reasonably well with the solution data (Δ = 0.03 Å), indicating minimal solvation effects on the strong U−O_t bond. The U−O_t distance found in solution (1.76 Å) is short compared with other experimental data for UO_2^{2+} in solution (1.76−1.78 Å);[20,21] in fact, one would expect a longer U−O_t bond in M1 because four aqua ligands of a completely solvated uranyl complex are replaced by stronger bound ligands, namely by two Cl ligands and two OH bridges. The polar U−Cl bond, however, is notably shorter than in solution (Δ = −0.26 Å) and may be elongated by screening effects and possible H bonds in solution. The calculated average distance (2.42 Å) of all equatorial U−O bonds is only 0.02 Å longer than the experimental value. The bridging bonds U−O_b and U−O_b' are significantly shorter than the bonds U−O_a and U−O_s (Δ ≈ −0.14 Å); indicating increased bond strengths of the linking bridges.

Before judging the gas-phase model M1 against the crystal data, we briefly compare the available experimental solution and crystal structure data. Overall, they are similar, with a tendency to longer bonds in the crystal, except for the U−Cl distance. This may be because the H bonds in solution are more flexible and dynamically changing than the localized crystal H bonds; thus, the corresponding bonds are weakened and lengthened in a more pronounced fashion. The average U−O distance in the crystal is 0.01 Å longer than in solution. The U−U and U−Cl distances though are noticeably different from solution, with Δ = 0.10 Å and −0.14 Å, respectively, indicative of a weakening of the bridging bonds due to H bonds in the crystal (A and F in Figure 2). Invoking bond order conservation at the two uranyl moieties, this weakening would lengthen the U−U distance and strengthen the other equatorial bonds, including the U−Cl bond.

Model M1 is in relatively good agreement with the crystal structure, particularly considering the experimental uncertainties. Only slight deviations are found for the U−O_b (Δ = −0.01 Å) and U−O_b' (Δ = −0.02 Å) distances; also, the correct order of these two distances is reproduced (U−O_b > U−O_b'). However, the U−U distance, which does not represent an actual bond (3.80 Å), is strongly underestimated (Δ = −0.14 Å), yielding a more compact complex than the crystal structure; this is probably due to the stronger bridging bonds. The bonds to the aqua ligands U−O_a and U−O_s are almost equal in model M1, with a slightly longer distance U−O_a (Δ = 0.01 Å), whereas the crystal U−O_s bond is significantly longer, by 0.11 Å. The distance U−O_a (Δ = 0.10 Å) is too long compared to experiment whereas that of U−O_s (Δ = −0.01 Å) agrees very well. This may be traced to the effects of the H bonds involved, i.e. A, B, C, and D for U−O_a whereas the U−O_s bond length is unaffected by any of the postulated H bonds (Figure 2). The underestimation of the U−Cl distance (−0.12 Å) can be rationalized with the missing weakening effects due to H bonds C and D. The linearity of the uranyl moieties is very well reproduced (Δ = −1.5°) and deviations of other characteristic angles are small, 3−5° (Table 1).

Before turning to the computational results for model M2, where H bonds are taken into account, we briefly discuss results obtained with the highly symmetric gas-phase model M0 of C_{2h} symmetry. Model M0 shows surprisingly good overall agreement with M1 (Table 1); as expected, the main differences are with the OH bridges which are not bent due to symmetry restrictions. In addition, the order of the two distances U−O_b and U−O_b' is reversed (U−O_b < U−O_b'). The reduction in U−O_b (Δ = −0.14 Å compared to model M1) gives a shorter U−U distance (Δ = −0.02 Å) and a weakening of the U−Cl bond (Δ = 0.07 Å) due to the stronger bridging bonds. Although the U−O_t bonds are only very slightly elongated (Δ = 0.005 Å), the uranyl units are more strongly bent, 169° compared to 177° in M1, whereas deviations of other angles range from 1 to 9°.

In model M2, the H bonds A, B, C, and D were simulated to account for the crystalline environment (Figure 3). Consequently, compared to model M1, most bonds are elongated. All bond lengths except U−O_b are improved in comparison to model M1 (Table 1), with deviations Δ from experiment ranging from less than 0.01 Å up to 0.09 Å; even the U−U distance is distinctly elongated (Δ = −0.07 Å). Agreement with experimental data for U−O_a (Δ = 0.03 Å) and U−Cl (Δ = −0.09 Å) is notably improved whereas the distance U−O_s (|Δ| < 0.01 Å) is hardly affected because O_s is not involved in an H bond. Unlike model M1, the correct ordering of the lengths of the two types of aqua ligand bonds U−O_a and U−O_s is reproduced (U−O_a < U−O_s). The calculated H bond Cl···H−O_a (D) is distinctly longer than the experimental bond (see below), which reduces the effect on the corresponding U−Cl bond; this may explain the relatively strong deviation from experiment calculated for the U−Cl distance (Δ = −0.09 Å). The effect of the H bonds A on the O_b atoms is significant: the distance U−O_b (Δ = −0.05 Å) changes by 0.04 Å, the bending angle of the O_b−H bond is reduced from 66.6° in model

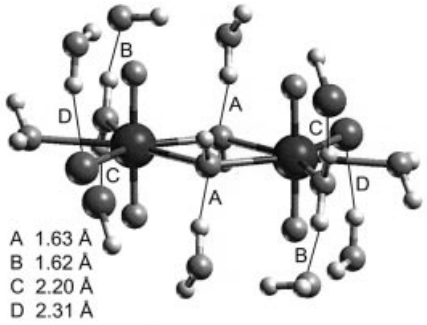

Figure 3. Optimized structure of the dinuclear complex $[(UO_2)_2(\mu_2\text{-}OH)_2Cl_2(H_2O)_4]$ (**1**), including simulated H bonds A, B, C, and D (model M2); also shown are calculated H···Y distances [Å]

M1 to 52.9°; the distance U−O_b' is less affected and changes by 0.025 Å. Both the angle O_t−U−O_t ($\Delta = -3°$) and the remaining angles ($\Delta = 1-5°$) agree well with experiment, with deviations of the same order as in model M1.

We also find very good agreement for the strong U−O_t bonds ($\Delta < 0.01$ Å), in fact for all models M0, M1 and M2. Thus, the postulated H bonds E and F seem to affect the uranyl bonding only weakly. This corroborates our decision to neglect these weak bonds in model M2. From previous results for similar systems,[14] the expected accuracy of about ±0.02 Å for bond lengths was not reached in model M2 for the U−O_b, U−O_a, and U−Cl bonds; however, inclusion of the most important H bonds in model M2 distinctly improved the results compared to model M1. Note that the crystal structure differs slightly from the C_i symmetry assumed for the computational models, resulting in a scattering of the experimental distances by up to ±0.04 Å; this is of the same order as experimental uncertainties (0.01−0.03 Å, Table 1). Thus, for most bonds, the remaining deviations are within experimental uncertainty, but may also partly be caused by the applied symmetry restriction and the lack of H bonds E and F in model M2.

The crystal structure provides limited information on H bonds, but from model M2 we can locate the hydrogen atoms involved and the angles of the simulated H bonds (Table 2, Figure 3). The calculated H bonds A ($\Delta = -0.02$ Å) and C ($\Delta = 0.04$ Å) are in good agreement with the X···Y distances found in the crystal; this is noteworthy as H bonds are not described with high accuracy with a local-density approximation of the exchange-correlation functional (see $\Delta = 0.07$ Å for the H bonds B and D).[22] The calculated Cl···O_a distance of bridge D is too long, which seems to indicate a weaker H bond in model M2 than expected from the crystal structure. As a consequence, the calculated U−Cl bond is less destabilized and too short (see above). The agreement of both chemical bond lengths and X···Y distances of H bonds, calculated for model M2, with the corresponding data of the crystal structure confirms that the relaxation of the gas-phase structure of complex **1** (M1) is properly described in the simulated crystalline environment of model M2.

Our computational results for H bonds can also be compared to typical data[17] for H···Y distances and X−H···Y angles (Table 2). Such comparison allows us to classify the H bonds A and B as relatively strong, both resulting in almost linear bonds with O_a−H···O_b angles of 173° (Table 2). For the H bonds C and D typical weak-to-moderate bonds are indicated, with elongated distances and O_a−H···Cl angles of 171 and 156°, respectively. Charge exchange from individual H bonds to the corresponding acceptor atoms in the complex is small; the total electronic charge donation of all eight H bonds is ca. 0.4 e compared to the gas-phase model M1. According to a Mulliken population analysis, there is a slight charge donation to centers O_b (0.04 e) and Cl (0.03 e) from the H bonds A and D and also from H bonds B and C to both H atoms in H_2O_a (0.03 and 0.06 e, respectively). The calculated charge donation of ca. 0.4 e is a deficiency of our model because the molecular crystal contains neutral units of **1**. A net donation of electron charge should usually result in an elongation of bonds. However, compared to experiment, the deviations of calculated bond lengths in model M2 are the same size as found for the dinuclear species $(UO_2)_2(OH)_2(H_2O)_6^{2+}$.[14] Thus, we are confident that potential artifacts due to a net charge of complex **1** are small.

In the additional models M2′ and M2′′ we also investigated relaxation effects of complex **1** that occur on removing the constraint that all equatorial ligand atoms of the uranyl moieties be confined to one plane (see above). As the crystal structure provides no evidence for H bonds to *syn*-aqua ligands, there is no predefined orientation of the corresponding hydrogen atoms, in contrast to those of the *anti*-aqua ligands (Figure 2). Therefore, while maintaining overall C_i symmetry during relaxation of the constraint, two isomers are possible. In the first model (M2′), the hydrogen atoms of the *syn*-aqua ligands are oriented as in model M2 (Figure 3); in the second model (M2′′), these ligands are rotated by about 180° around the U−O_s bond.

Table 3 gives the geometries of the two structures M2′ and M2′′ compared with that of model M2. At first sight, the structures of the three models are very similar. Deviations between the three models are generally < 0.02 Å for distances and < 3° for angles. The most prominent geo-

Table 2. Bond lengths [Å], angles [°], and binding energies (*BE*) [kJ/mol] of modeled H bonds A, B, C, and D of model M2 in comparison with the crystal structure (in parentheses) and typical values for H bonds of various strengths; frontier groups of adjacent complexes $[(UO_2)_2(\mu_2\text{-}OH)_2Cl_2(H_2O)_4]$ (**1**) are designated in *italics*

			X···Y[a]	H···Y	X−H···Y	*BE*[b]
M2	A	O_a−*H*···O_b	2.630 (2.65)	1.632	173.2	84
	B	O_a−H···*O_b*	2.648 (2.58)	1.615	173.3	113
	C	O_a−H···*Cl*	3.177 (3.14)	2.197	171.1	14
	D	O_a−*H*···Cl	3.233 (3.16)	2.310	156.0	27
Typical values[c]		strong	2.2−2.5	1.2−1.5	175−180	60−170
		moderate	2.5−3.2	1.5−2.2	130−180	20−70
		weak	3.2−4.0	2.2−3.2	90−180	< 20

[a] Experimental values (ref.[2]) of crystal structure in parentheses. [b] Binding energies calculated from **1** (M2) → **1** (M2 − 2X) + 2X, X = H_2O for A, B, D and X = HCl for C (see text). [c] Ref.[17], typical values from various compounds.

Table 3. Selected structure parameters (distances in Å) and stability ΔE (relative to M2, in kJ/mol) of C_i-symmetric models M2, M2′ and M2′′ (see text) of complex $[(UO_2)_2(\mu_2\text{-}OH)_2Cl_2(H_2O)_4]$ (**1**), in a model of the crystalline environment; also shown are experimental values of the structure parameters (for the designations, see Figure 2 and text)

	U−U	U−O_b	U−O_b′	U−O_a	U−O_s	U−Cl	ΔE
M2	3.875	2.352	2.343	2.421	2.497	2.661	−
M2′	3.883	2.353	2.348	2.406	2.499	2.665	−7
M2′′	3.880	2.337	2.363	2.411	2.486	2.668	12
Exp.[a]	3.94(0)	2.40(2)	2.34(2)	2.39(2)	2.50(3)	2.75(1)	

[a] Ref.[2], crystal structure (average values with respect to the assumed C_i symmetry; maximum scattering of 0.04 Å for distances and 1.7° for angles).

metrical difference relates to the U−O_b and U−O_b′ distances. Model M2′ agrees very well with model M2, concerning both length of the two bridges and their ordering (U−O_b > U−O_b′). A major improvement compared to experiment is the shortening of U−O_a by 0.02 Å (Table 3). Conversely, in model M2′′, U−O_b decreases by 0.02 Å whereas U−O_b′ increases by 0.02 Å compared to model M2; therefore the ordering of the two bridges disagrees with experiment: U−O_b < U−O_b′. Thus, also taking into account small energy disadvantages of ΔE = 12 and 19 kJ/mol over M2 and M2′, respectively, we rule out model M2′′ (Table 3).

Although model M2′ is calculated to be slightly more stable than M2 (by 7 kJ/mol; Table 3), the H bond structure favors M2 over M2′. In model M2′, the X···Y distances of the weak-to-moderate bonds C (Δ = 0.21 Å) and D (Δ = 0.19 Å) are significantly longer than in experiment; they are also overestimated in model M2 (C: Δ = 0.04 Å; D: Δ = 0.07 Å), but to a considerably smaller extent. The X···Y distances of the strong H bonds (A: Δ = −0.02 Å; B: Δ = −0.04 Å) remain similar to model M2 (see above), and the angles X−H···Y are only slightly affected, with changes below 2°. Yet, the structural relaxation of model M2′, where the equatorial ligands bend slightly out of the equatorial plane, results in notable changes in H bond lengths and removes the good agreement of the H bond network calculated for model M2 with the crystal structure.

In summary, we favor model M2 and M2′, and exclude model M2′′ based on structure and energy arguments. M2 and M2′ are very similar if one considers the internal structure of **1**. We note that the H bonds of model M2′ fit the experiment less well. These bonds are rather flexible and thus they change strongly with small geometry alterations of the central complex. Nevertheless the differences between models M2 and M2′ should not be over-interpreted, keeping in mind the approximate modeling of the crystalline environment of **1**.

Energetics

To compare the relative energies of our models, we chose the low symmetry gas-phase model M1 (C_i symmetry) as reference. Model M0, where out-of-plane bending of the OH bridges is prevented by the imposed C_{2h} symmetry, is 47 kJ/mol less stable. Contrary to this relatively small energy change, model M2 is 315 kJ/mol more stable due to the simulated eight H bonds. This calculated stabilization energy was based on the reaction **1** (M1) + 6 H_2O + 2 HCl → **1**·6H_2O·2HCl (M2). With respect to the eight H bonds formed, this energy translates into an average binding energy of 39 kJ/mol per H bond, which falls in the range 20−70 kJ/mol that is typical for moderately strong H bonds,[17] thus corroborating the previously discussed structural evidence concerning their strength.

To estimate the strengths of individual H bonds, we removed the corresponding frontier groups from model M2 and considered the model reaction **1** (M2) → **1** (M2 − 2 X) + 2 X where X = H_2O for the H bonds A, B, and D and X = HCl for H bond C. No structure relaxation was allowed. The energies of the H bonds A, B, C, and D thus estimated are 84, 113, 14, and 27 kJ/mol, respectively (Table 2). These calculated energies confirm the previous classification of the H bonds based on structural evidence: H bonds A and B, with average binding energies of about 99 kJ/mol, represent typical strong H bonds (60−170 kJ/mol)[17] whereas H bonds C and D are significantly weaker, with average binding energies of about 21 kJ/mol. Together with the good overall agreement of the detailed geometry of model M2 with the crystal structure, these energy results confirm that the simulated H bonds represent the main crystal packing effects.

Conclusion

A scalar relativistic density functional method as implemented in the parallel code PARAGAUSS was employed to study the structure of the hexavalent dinuclear uranyl chloride complex $[(UO_2)_2(\mu_2\text{-}OH)_2Cl_2(H_2O)_4]$ (**1**) in the gas phase as well as in its crystalline environment. A local-density approximation of the exchange-correlation functional was used for the geometry optimization; energies were determined with a generalized-gradient approximation (see below).

We applied different models to describe both the gas-phase structure and packing effects in the molecular crystal. The gas-phase reference model agrees reasonably well with the experimental structure; major deviations are due to the neglect of H bonds of the crystal environment. Notable deviations occur for U−O distances of an aqua ligand (too long by 0.10 Å) and U−Cl bonds (too short by 0.12 Å). We also found surprisingly good agreement for an initial high-symmetry model which enforced coplanarity of the OH bridges.

We described H bonds in the crystal environment via model H_2O and HCl moieties that mimic the effect of frontier groups of neighboring complexes **1**. In this model, the calculated structure is significantly improved. Average deviations from experiment are reduced from 0.04 to 0.03 Å for bond lengths (maximum deviation 0.09 Å for U−Cl) and from 3.5 to 2.6° for angles (maximum deviation 5°). One

can imagine a still further improved model that includes all postulated H bonds.

Based on this model, the lengths and angles of the hydrogen bonds were determined, indicating moderate and strong H bonds with an average binding energy of 39 kJ/mol. These computational results corroborate earlier suggestions, based on experimental results, concerning the location and strength of H bonds. The good agreement of both geometry and H bonds with the crystal structure confirms the correct orientation of the complex in the simulated crystalline environment and justifies our model approach.

Computational Details

Scalar relativistic all-electron calculations were carried out by the LCGTO-FF-DF method[23] (linear combination of Gaussian-type orbitals fitting function density functional) as implemented in the parallel code PARAGAUSS.[24,25] The relativistic density functional method applied is based on the second-order Douglas-Kroll-Hess (DKH) approach[26,27] to the Dirac-Kohn-Sham problem.[7,28] Besides the standard scalar relativistic variant, a two-component version is available that includes spin-orbit interaction self-consistently.[29] Due to the closed-shell electronic structure of the U^{VI} species examined we refrained from including spin-orbit interaction.

We employed two exchange-correlation functionals: the local-density approximation (LDA) in the parameterization of Vosko, Wilk, and Nusair (VWN),[30] and the gradient-corrected functional (generalized gradient approximation, GGA) suggested by Becke and Perdew (BP).[31,32] Structures were optimized at the LDA level, invoking a quasi-Newton algorithm and analytical forces.[33,34] The LDA often yields more accurate results for molecular geometries, whereas gradient-corrected functionals perform better for binding energies.[35,36] Therefore, we applied the BP functional self-consistently to calculate binding energies at the structures optimized with the VWN functional.

The Kohn-Sham orbitals were represented by flexible Gaussian-type basis sets, contracted in a generalized fashion using atomic eigenvectors. For U, we used a basis set of the size (24*s*, 19*p*, 16*d*, 11*f*),[37] contracted to [10*s*, 7*p*, 7*d*, 4*f*]. The light atoms (Cl, O, H) were described by standard basis sets:[38] (12*s*, 9*p*, 1*d*) → [6*s*, 5*p*, 1*d*] for Cl, (9*s*, 5*p*, 1*d*) → [5*s*, 4*p*, 1*d*] for O, and (6*s*, 1*p*) → [4*s*, 1*p*] for H. To evaluate the classical Coulomb contribution to the electron-electron interaction in the LCGTO-FF-DF method, the electron density is represented with the help of an auxiliary basis set.[23] The exponents of the corresponding *s*- and r^2-type fitting functions were generated from the orbital basis by a standard procedure;[23] in addition, we chose *p*-, *d*- and *f*-type "polarization exponents" as geometric series with a factor 2.5, starting with 0.1, 0.2 and 0.3 for *p*-, *d*- and *f*-type exponents, respectively. Thus, for U, the auxiliary charge density basis set was of the size (24*s*, 9r^2, 5*p*, 5*d*, 5*f*); the auxiliary basis sets for Cl, O, and H were (12*s*, 9r^2, 5*p*, 5*d*), (9*s*, 5r^2, 5*p*, 5*d*), and (6*s*, 1r^2, 5*p*), respectively. Recently, we checked the quality of the auxiliary basis sets for uranyl; comparison with other DF calculations confirmed the accuracy of the current FF approach for actinide complexes.[39]

In the geometry optimizations, the total energy and elements of the density matrix were required to converge to 10^{-8} au; for the largest component of the displacement gradient vector and the update step length, the convergence criteria were set to 10^{-6} au. For model M1, the grid[40] for the numeric integration of the exchange-correlation functional consisted of about 26200, 16000, 10000, and 8900 points for U, Cl, O, and H centers, respectively.

Previous studies of various hexavalent actinide compounds,[39] including the dinuclear uranium species $[(UO_2)_2(OH)_2(H_2O)_x]^{2+}$ and $[(UO_2)_2O_2(H_2O)_x]$ (x = 0, 2, 4, 6),[14] showed that the computational strategy just described yields very satisfactory results. The LDA (VWN) functional provided accurate bond lengths and vibrational frequencies. Results obtained with uncontracted and contracted basis sets agreed rather well; for the dinuclear species[14] bond lengths differed by at most 0.002 Å, angles by at most 0.2° and binding energies by at most 2 kJ/mol; for mononuclear compounds,[39] deviations of distances were less than 0.0006 Å.

Acknowledgments

This work was supported by the German Bundesministerium für Wirtschaft (grant no. 02E9450) and the Fonds der Chemischen Industrie.

[1] M. Åberg, *Acta Chem. Scand.* **1970**, *24*, 2901−2915.
[2] M. Åberg, *Acta Chem. Scand.* **1969**, *23*, 791−810.
[3] A. Navaza, F. Villain, P. Charpin, *Polyhedron* **1984**, *3*, 143−148.
[4] J. Toivonen, R. Laitinen, *Acta Crystallogr., Sect. C* **1984**, *40*, 7−14.
[5] P. B. Viossat, N.-H. Dung, E. C. Soye, *Acta Crystallogr., Sect. C* **1983**, *39*, 573−579.
[6] M. Pepper, B. E. Bursten, *Chem. Rev.* **1991**, *91*, 719−741.
[7] N. Rösch, S. Krüger, M. Mayer, V. A. Nasluzov, in *Theoretical and Computational Chemistry*, vol. 4 ("Recent Developments and Applications of Modern Density Functional Theory") (Ed.: J. Seminario), Elsevier, Amsterdam, **1996**, p. 497−566.
[8] G. Schreckenbach, P. J. Hay, R. L. Martin, *J. Comp. Chem.* **1999**, *20*, 70−90.
[9] V. Vallet, U. Wahlgren, B. Schimmelpfennig, H. Moll, Z. Szabó, I. Grenthe, *Inorg. Chem.* **2001**, *40*, 3516−3525.
[10] T. Privalov, B. Schimmelpfennig, U. Wahlgren, I. Grenthe, *J. Phys. Chem. A* **2003**, *107*, 587−592.
[11] S. Spencer, L. Gagliardi, N. C. Handy, A. G. Ioannou, C.-K. Skylaris, A. Willets, A. M. Simper, *J. Phys. Chem. A* **1999**, *103*, 1831−1837.
[12] S. Tsushima, T. Yang, A. Suzuki, *Chem. Phys. Lett.* **2001**, *334*, 365−373.
[13] P. Pyykkö, *Chem. Rev.* **1988**, *88*, 563−597.
[14] F. Schlosser, M. Fuchs-Rohr, S. Krüger, N. Rösch, to be published.
[15] F. A. Cotton, G. Wilkinson, in *Advanced Inorganic Chemistry*, 5th ed., John Wiley & Sons, New York, **1988**, p. 980−993.
[16] K. A. Gschneidner, L. Eyring, G. R. Choppin, G. H. Lander, *Handbook on the Physics and Chemistry of Rare Earths*, vol. 18

("Lanthanides/Actinides: Chemistry"), North-Holland, Amsterdam, **1994**, p. 529−558.
[17] G. A. Jeffrey, *An Introduction to Hydrogen Bonding*; Oxford University Press, New York, **1997**, p. 12.
[18] R. C. Weast, *CRC Handbook of Chemistry and Physics*, 59th ed., CRC Press, Boca Raton, **1979**, p. D-230.
[19] M. Fuchs, A. Shor, N. Rösch, *Int. J. Quant. Chem.* **2002**, *86*, 487−501.
[20] P. G. Allen, J. J. Bucher, D. K. Shuh, N. M. Edelstein, T. Reich, *Inorg. Chem.* **1997**, *36*, 4676−4683.
[21] U. Wahlgren, H. Moll, B. Schimmelpfennig, L. Maron, V. Vallet, O. Gropen, *J. Phys. Chem. A* **1999**, *103*, 8257−8264.
[22] W. Koch, M. C. Holthausen, *A Chemist's Guide to Density Functional Theory*; Wiley-VCH, Weinheim **2000**, p. 213−234.
[23] B. I. Dunlap, N. Rösch, *Adv. Quantum Chem.* **1990**, *21*, 317−339.
[24] T. Belling, T. Grauschopf, S. Krüger, M. Mayer, F. Nörtemann, M. Staufer, C. Zenger, N. Rösch, in *High Performance Scientific and Engineering Computing* (Eds.: H.-J. Bungartz, F. Durst, C. Zenger), Lecture Notes in Computational Science and Engineering, Springer, Heidelberg, **1999**, vol. 8, p. 439−453.
[25] T. Belling, T. Grauschopf, S. Krüger, F. Nörtemann, M. Staufer, M. Mayer, V. A. Nasluzov, U. Birkenheuer, A. Shor, A. Matveev, A. Hu, N. Rösch, PARAGAUSS, version 2.1, Technische Universität München, **1999**.
[26] M. Douglas, N. M. Kroll, *Ann. Phys.* **1974**, *82*, 89−155.
[27] G. Jansen, B. A. Hess, *Phys. Rev. A* **1989**, *39*, 6016−6017.
[28] O. D. Häberlen, N. Rösch, *Chem. Phys. Lett.* **1992**, *199*, 491−496.
[29] M. Mayer, S. Krüger, N. Rösch, *J. Chem. Phys.* **2001**, *115*, 4411−4423.
[30] S. H. Vosko, L. Wilk, M. Nusair, *Can. J. Phys.* **1980**, *58*, 1200−1211.
[31] A. D. Becke, *Phys. Rev. A* **1988**, *38*, 3098−3100.
[32] J. P. Perdew, *Phys. Rev. B* **1986**, *33*, 8822−8824; J. P. Perdew, *Phys. Rev. B* **1986**, *34*, 7406.
[33] V. A. Nasluzov, N. Rösch, *Chem. Phys.* **1996**, *210*, 413−425.
[34] F. Nörtemann, Dissertation, Technische Universität München, **1998**.
[35] T. Ziegler, *Chem. Rev.* **1991**, *91*, 651−667.
[36] A. Görling, S. B. Trickey, P. Gisdakis, N. Rösch, in *Topics in Organometallic Chemistry*, vol. 4 (Eds.: J. Brown, P. Hoffmann), Springer, Heidelberg, **1999**, p. 109−165.
[37] T. Minami, O. Matsuoka, *Theor. Chim. Acta* **1995**, *90*, 27−39.
[38] Cl: *s* and and *p* exponents from: A. Veillard, *Theor. Chim. Acta (Berlin)* **1968**, *12*, 405−411; *d* exponent (0.56) from: Y. Sakai, H. Tatewaki, S. Huzinaga, *J. Comput. Chem.* **1981**, *2*, 108−125. O: *s* and *p* exponents from: F. B. Van Duijneveldt, *IBM Res. Rep.* **1971**, RJ 945; *d* exponent (1.15) from: S. Huzinaga, J. Andzelm, M. Klobukowski, E. Radzio-Andzelm, Y. Sakai, H. Tatewaki, *Gaussian Basis Sets for Molecular Calculations*, Elsevier, Amsterdam, **1984**; H: *s* exponent from: F. B. Van Duijneveldt, *IBM Res. Rep.* **1971**, RJ 945; *p* exponent (1.0) from: M. J. Frisch, J. A. Pople, J. S. Binkley, *J. Chem. Phys.* **1984**, *80*, 3265−3268.
[39] M. García-Hernández, C. Lauterbach, S. Krüger, A. Matveev, N. Rösch, *J. Comp. Chem.* **2002**, *23*, 834−846.
[40] A. D. Becke, *J. Chem. Phys.* **1988**, *88*, 2547−2550.

Received January 14, 2003

